EXPERT OPINION

informa
healthcare

Isolation and characterization of the human immature osteoblast culture system from the alveolar bones of aged donors for bone regeneration therapy

Makoto Aino, Eisaku Nishida, Yoshiyasu Fujieda, Ai Orimoto, Akio Mitani, Toshihide Noguchi, Hatsune Makino, Shinya Murakami, Akihiro Umezawa, Toshiyuki Yoneda & Masahiro Saito†

†*Tohoku University Graduate School of Dentistry, Division of Operative Dentistry, Department of Restorative Dentistry, Sendai, Japan*

Background: Establishment of human osteoblast cultures that retain bone-forming capacity is one of the prerequisites for successful bone regeneration therapy. Because osteoblasts harvested from adults exhibit limited growth, the use of immature osteoblasts that can expand *ex vivo* should greatly facilitate bone regeneration therapy. In this study, we developed immature human osteoblasts isolated from aged alveolar bone (HAOBs).

Methods: HAOBs obtained after the collagenase digestion of alveolar bones from elderly donors. Then, we assessed osteogenic ability of HAOB after treatment with recombinant human bone morphogenic protein-2 or transplantation into immunodeficient mice. In addition, we performed global gene expression analysis to identify functional marker for HAOB.

Results: HAOBs, which can differentiate into osteoblasts and have a robust bone-forming ability, were successfully extracted from donors who were > 60 years of age. We found that the HAOBs exhibited a higher osteogenic ability compared with those of human mesenchymal stem cells and highly expressed *NEBULETTE (NEBL)* with osteogenic abilities.

Conclusions: HAOBs have properties similar to those of human immature osteoblasts and appear to be a novel material for cell-based bone regeneration therapy. Additionally, the expression level of *NEBL* may serve as a marker for the osteogenic ability of these cells.

Keywords: aging, bone morphogenic protein, bone regeneration, human immature osteoblast, NEBULETTE

Expert Opin. Biol. Ther. (2014) 14(12):1731-1744

1. Introduction

Human bone regeneration appears to be limited in its ability to repair large bone defects associated with tumor resection or comminuted open fractures [1]. Thus, a bone regeneration strategy that yields functional and mechanically competent bone is necessary [2,3]. Autogenic bone grafting has been used for bone substitution and repair; however, the limited availability of donor bone and the additional surgical procedure required to procure tissue are major limitations associated with bone autografting [4]. Because of these problems, bone tissue engineering has been developed as an alternative strategy for bone regeneration [3,5]. Because of their osteogenic potential, mesenchymal stem cells (MSCs) are expected to serve as a cell source for the regeneration of critical bone defects [6]. Although bone regeneration

10.1517/14712598.2014.960387 ISSN 1471-2598, e-ISSN 1744-7682

mediated by MSCs shows potential utility, large variations have been observed in the bone-forming ability of human MSC cells, and their osteogenic potential is gradually lost upon *ex vivo* expansion [7]. In addition, healing calvarial bone defects using MSC requires the exogenous expression of growth factors, usually using viral transfer [8,9].

In addition to the effort to increase bone-forming ability by MSCs *in vivo*, the use of immature osteoblasts as a potential cell source for bone regeneration has been investigated [10]. The transplantation of primary juvenile immature osteoblasts obtained from murine calvaria or murine osteoblast cell lines is capable of healing calvarial bone defects without the exogenous expression of growth factors. Because bone tissue engineering is generally approached using a combination of osteogenic cells and biodegradable scaffolds [11-13], immature osteoblasts may be a promising cell source for bone regeneration therapy [14,15].

Osteoblasts are bone-forming cells derived from multipotent MSCs. During skeletal development, multipotent MSCs become osteoblast progenitor cells and undergo commitment into immature osteoblasts, which express alkaline phosphatase (ALP) and type I collagen through the action of RUNX2 and osterix [16]. Immature osteoblasts are capable of proliferating before becoming mature osteoblasts [3]. Although mature osteoblasts can synthesize and deposit bone extracellular matrix components such as osteocalcin (OCN) and bone sialoprotein (BSP), their ability to proliferate is greatly reduced [16]. Thus, recapitulating immature osteoblast differentiation has been suggested as a promising approach for bone regeneration therapy [17]. Previous studies demonstrated that primary osteoblast cultures from newborns contained large numbers of immature osteoblasts, and these cells were able to expand and were capable of healing critical bone defects [14,15]. However, the cells isolated from adult bone showed limited cell division and low osteogenic differentiation ability, likely due to the reduction of immature osteoblasts caused by age [18]. Thus, the development of new culture techniques to expand adult immature osteoblasts *ex vivo* is important for the achievement of bone regeneration therapy [19].

The alveolar bone is the part of maxilla and mandible that forms and supports the sockets of teeth and originates from dental follicles that contain stem cells capable of differentiating into periodontal tissue, including the periodontal ligament and cementum [20]. In contrast, skeletal bone exists throughout the entire body, except for the craniofacial bone, and is formed by membranous ossification or endochondral ossification. Like skeletal bone, alveolar bone undergoes constant remodeling in response to tooth eruption and the forces of mastication, suggesting a resemblance to skeletal bone [21]. Several studies have shown that human alveolar bone cells were easily accessible during routine oral surgical procedures. Cultured alveolar bone cells exhibit ALP activity and resemble osteoblasts [22-24]. Explant cultures from human alveolar bone that were seeded into three-dimensional type I collagen scaffolds were shown to induce new bone tissue when implanted into critical-size bone defects in the skulls of immunodeficient (SCID) mice [22]. Additionally, bone marrow stromal cells obtained from alveolar bone during oral surgery were found to have a potent osteogenic potential that was comparable to stromal cells obtained from the iliac crest, suggesting that alveolar bone cells may possess features that resemble osteoblasts located in skeletal bone [25]. These findings strongly indicate that human alveolar bone can serve as a useful cell source for isolating bone-forming cells required in bone regeneration therapy.

In the present study, protocols for expanding and harvesting these cells were investigated to identify more efficient culture conditions for immature osteoblasts obtained from the alveolar bones of middle-aged patients. Both *in vitro* and *in vivo* bone formation results showed that this system is an effective means by which to enrich and expand human immature osteoblasts, and these modifications have resulted in the induction of *in vivo* bone formation and the identification of NEBL as a marker for osteoinductive cells.

2. Methods

2.1 Isolation of human alveolar bone osteoblasts

Human alveolar bone was obtained from 62-, 55-, 52- and 27-year-old subjects during surgical resection. The experimental procedures were approved by the Ethical Committees of Kanagawa Dental College (approval #30) and the Osaka University School of Dentistry (approved #H20-E2), and all subjects provided written informed consent prior to the study. Human alveolar bone particles (5 mm^2) were sequentially digested with 3 mg/ml bacterial collagenase (Roche Diagnostics, Penzberg, Germany) in PBS. Eight populations were obtained: two after a 10-min digestion, one after a 20-min digestion and five after a 40-min digestion. The first three populations were discarded, and the last five were incubated in 35-mm dishes with MF start medium (Toyobo Life Technology, Osaka, Japan) in a humidified atmosphere of 5% CO_2 at 37°C. These cells were passaged using PBS containing 0.25% trypsin·mmol/l EDTA when they reached ~ 80% confluence, and they were maintained as human alveolar bone osteoblasts (HAOBs). HAOBs were plated into six wells at a density of 3×10^4 cells/ml with MF medium (Toyobo Life Technology), and the medium was changed every 2 days. After incubation for 5 days, the HAOBs were evaluated for ALP activity, calcium accumulation by alizarin red staining and mRNA expression of bone markers as described below. For comparison, normal human foreskin fibroblasts (HFFs) were purchased from Lonza (Allendale, NJ, USA) and maintained in MF medium. Each cell population doubling (PD) was calculated using a previously published method [26].

2.2 *In vivo* differentiation assay

The implantation of HAOBs into SCID mice was conducted as previously described [27]. Briefly, cells were inoculated subcutaneously into 5-week-old male CB-17 scid/scid (SCID)

mice (Nihon Crea, Tokyo, Japan) after incubating 1.5×10^6 cells in a mixture of 40 mg of hydroxyapatite powder (OSferion; Olympus, Tokyo, Japan) and fibrin clot, a mixture of mouse fibrinogen and thrombin, (Sigma, St. Louis, MO). A transplantation analysis was carried out three times, and three transplants were prepared per group that either had implanted HAOBs or was without cells. Four weeks after implantation, the transplants were bisected, and the halves were used for examination by histochemical and mRNA expression analyses of osteogenic genes as described above. For histochemical analysis, the transplants were fixed in 4% paraformaldehyde for 1 day, decalcified with 10% formic acid for 3 days and then embedded in paraffin. Subsequently, 3-µm-thick serial sections were prepared per implant and subjected to immunohistochemical analysis as described below.

2.3 Histochemical analysis

Sections of HAOB transplants were prepared as described above. To avoid the nonspecific staining of mouse monoclonal antibodies in the transplants, the sections were blocked using the M.O.M. kit (Vector Laboratories, Burlingame, CA, USA) as previously described [27]. The sections were incubated with an anti-human OCN polyclonal antibody (FL-100, Santa Cruz Biotechnology, Inc., TX 75220, USA), an anti-human OSTEOPONTIN (OPN) polyclonal antibody (O-17, Immuno-Biological Laboratories Co., Ltd., Takasaki, Japan) and mAb V9 for 1 h and treated with biotinylated secondary antibody and avidin-peroxidase conjugate. Dilutions were made with PBS containing 1 mg/ml bovine serum albumin (BSA). The colorimetric reaction was developed using diaminobenzidine.

The cells were fixed with 4% paraformaldehyde and blocked with 1% BSA. The primary antibodies that were used were anti-human OCN monoclonal antibody (clone; GluOC4-5, Takara Bio Inc., Tokyo, Japan) and anti-human OPN polyclonal antibody (O-17, Immuno-Biological Laboratories Co., Ltd., Takasaki, Japan). The secondary antibodies that were used were Alexa Fluor 555 anti-rabbit IgG and Alexa Fluor 488 anti-mouse IgG (Invitrogen Corp.) followed by nuclear staining with 4′,6-Diamidino-2-phenylindole dihydrochloride. Fluorescent images were collected sequentially using a confocal microscope featuring 430-, 488- and 555-nm laser lines (LSM510; Carl Zeiss, Oberkochen, Germany).

2.4 G-banding karyotypic analysis

G-band karyotypic analysis was performed to assess the safety of *ex vivo* expansion of HAOB. Metaphase spreads were prepared from cells treated with colcemid (Karyo Max; Gibco BRL; 100 ng/ml for 6 h). We performed a standard G-banding karyotypic analysis on at least 50 metaphase spreads for each population.

2.5 Spectral karyotyping analysis

Spectral karyotyping (SKY) was performed on metaphase-transduced HAOBs after 35 PDs according to the manufacturer's instructions (ASI, Carlsbad, CA, USA) and a previously published method [28].

2.6 Osteogenic differentiation

Cells were plated into six wells at a density of 3×10^4 cells/ml and cultured in osteogenic differentiation medium such as MF medium supplemented with 100 ng/ml recombinant human bone morphogenic protein (rhBMP)-2, 100 nM dexamethasone, 50 µg/ml ascorbic acid and 10 mM β-glycerophosphate. The culture medium was replaced every 2 days, and the cells were maintained for 9 days. To compare the synthesis of osteogenic marker proteins, HAOBs were grown in osteogenic differentiation medium for 3 days and subjected to immunocytochemical analysis as described below.

2.7 ALP activity and alizarin red staining

To evaluate ALP activity, HAOBs were fixed with 4% paraformaldehyde for 20 min at 21°C. After being washed with PBS, the cells were stained with nitroblue tetrazolium (Sigma, St. Louis, MO) and 5-bromo-4-chloro-3-indolyl phosphate (Sigma, St. Louis, MO). ALP activity was measured as previously described [29]. Calcium accumulation was detected by staining preparations with 1% alizarin red solution for 5 min [29,30].

2.8 RNA isolation and real-time PCR analysis

Total RNA was isolated from cells using ISOGEN (Nippon Gene Co., Ltd., Tokyo, Japan) as previously described [27]. cDNA was synthesized from 1 µg of total RNA in a 20-µl reaction volume containing 10 × reaction buffer, 1 mM dNTP mixture, 1 U/µl RNase inhibitor, 0.25 U/µl reverse transcriptase (M-MLV reverse transcriptase, Invitrogen Corp., Carlsbad, CA, USA) and 0.125 µM random 9-mers (Takara, Tokyo, Japan). Real-time polymerase chain reaction (RT-PCR) was performed using Power SYBR® Green PCR Master Mix (Applied Biosystems, Carlsbad, CA, USA), and products were detected using an ABI 7300 Real-Time PCR System (Applied Biosystems). The primers for OSTERIX (forward, 5′-ctgaagaatgggtggggaagg-3′; reverse, 5′-ggcctctgtcctcctagctc-3′), RUNX2 (forward, 5′-gaaactcaacagattaactatcgtttgc-3′; reverse, 5′-gaatttatcacagatggtccctaatgg-3′), (OCN, forward, 5′-cacactcctcgccctattgg-3′; reverse, 5′-tgcacctttgctggactctg-3′), BSP (forward, 5′-cgaatacacgggcgtcaatg-3′; reverse, 5′-gtagctgtactcatcttcataggc-3′), NEBULETTE (NEBL) (forward, 5′-cattcccaaggctatggcta-3′; reverse, 5′-acgatgtagtcgccgtctct-3′), β-ACTIN (forward, 5′-gatgtatgaaggcttttggtctcc-3′; reverse, 5′-ctggtctcaagtcagtgtacagg-3′) and GAPDH (forward, 5′-gtcagtggtggacctgacct-3′; reverse, 5′-tcgctgttgaagtcagagga-3′) have been previously described.

2.9 GeneChip analysis

GeneChip analysis was performed as previously described [30]. Genome-wide gene expression was examined using the Human Genome U133A Probe array (GeneChip; Affymetrix, Santa Clara, CA, USA), which contains oligonucleotide probe

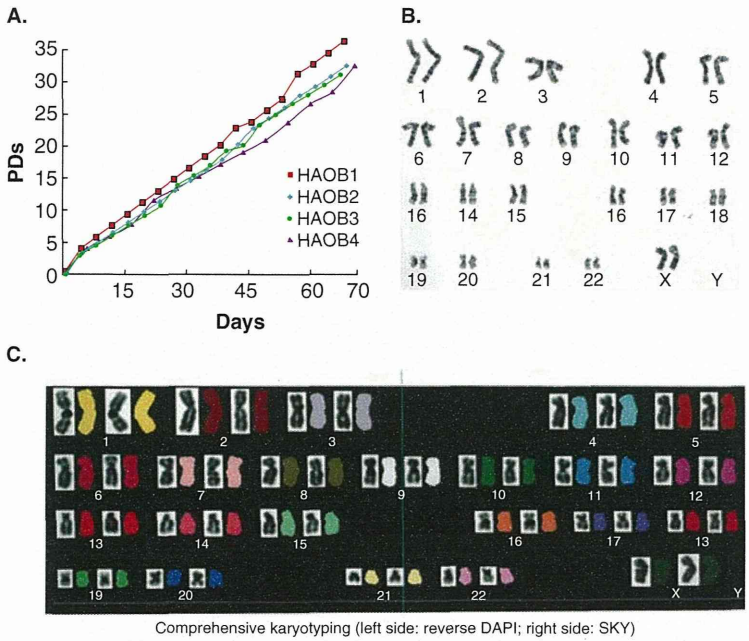

Figure 1. *Ex vivo* expansion of HAOBs. **(A)** Population doublings (PDs) of HAOBs obtained from patients of various ages (HAOB1-4) are shown. HAOBs obtained from the middle-aged donors (HAOB1-3) proliferated for > 30 PDs. The growth potential of these HAOBs is comparable to that of the HAOBs obtained from the young donors (HAOB4). Karyotypic analysis of HAOB3s at 35 PDs. **(B)** G-banded karyotyping and **(C)** spectral karyotyping were performed at metaphase, and chromosomal structures were determined in the indicated PDs. Normal diploidy was observed in representative HAOB3s.
HAOBs: Human alveolar bone osteoblasts.

sets for ~ 23,000 full-length genes and expressed sequence tags, according to the manufacturer's protocol (Expression Analysis technical manual and GeneChip Small Sample Target Labeling Assay version 2 technical note [http://www.affymetrix.com/support/technical/index.affx]). Data analysis was performed using the GeneChip Operation System (Affymetrix) and GeneSpringGX software (Silicon Genetics, Redwood, CA, USA). To normalize the staining intensity variations among chips, the average difference in values for all genes on a given chip were divided by the median of all measurements on that chip. Principal component analysis (PCA) was performed using the singular value decomposition method, which generates eigenvectors both for rows and columns of the log-transformed data matrix.

2.10 Knockdown experiment

HAOBs were transfected with Stealth siRNA (Invitrogen) using Lipofectamine RNAi MAX according to the manufacturer's protocol. Two sets of NEBL siRNA (5′-CCUUCGAGCC AAGAGGACAUCUGAA-3′ and 5′-UUCAGAUGUCCU-CUUGG CUCGAAGG-3′) were used to knockdown NEBL. Control siRNA was purchased from Invitrogen.

2.11 Statistical analysis

Statistical analyses were performed using SPSS software (Statistical Package for the Social Sciences, v. 15.0 J for Windows; SPSS, Chicago, IL, USA). The data are expressed as the mean ± s.e.m. Student's *t*-test was used for comparisons. Significance was accepted at $p < 0.05$.

3. Results

3.1 Isolation of HAOBs

We previously demonstrated the sequential digestion methodology for bovine alveolar osteoblasts that was used to establish an HAOB cell culture. In our preliminary experiments, Dulbecco's modified Eagle's medium (DMEM) or α-minimum essential medium (α-MEM) was used; however, the HAOBs were unable to expand *in vitro* due to viable cells in the alveolar bone possibly exhibiting a low proliferating activity. To overcome this problem, we selected MF-start™ to readily obtain an initial outgrowth of cells with a low proliferating activity during the primary culture. Alveolar bone tissues from different donor ages were digested with bacterial collagenase successively for various time periods as described in the Materials and Methods section. To identify the appropriate medium for the *ex vivo* expansion of HAOBs, we used several types of culture medium, including DMEM with 20% FCS, MSC basal medium (Lonza Walkersville, Inc., Allendale, NJ, USA) and MF start medium. MF start medium allowed for the expansion of the HAOBs from all donors (data not shown).

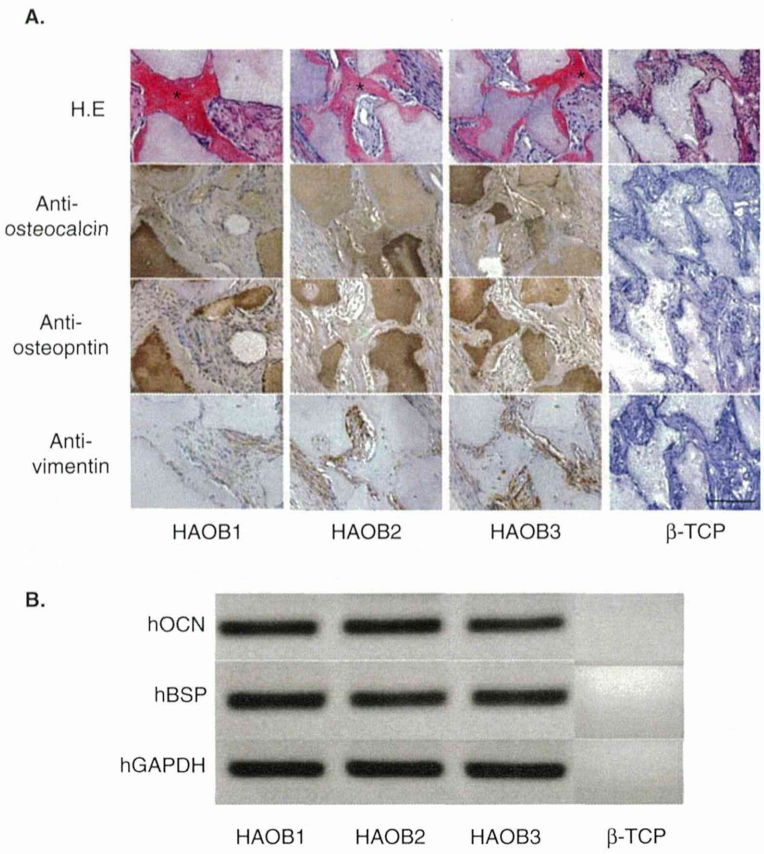

Figure 2. *In vivo* bone-forming ability of HAOBs. (**A**) The *in vivo* differentiation ability of HAOBs is shown. Representative sections of HAOB1-3 transplants and transplants without human cells were examined by hematoxylin and eosin staining (upper panel) or were immunostained with a human OCN antibody, human OPN antibody or human-specific vimentin antibody. The anti-osteocalcin- and osteopontin-positive bone-like tissue deposited in the HAOB cell transplants. The asterisk indicates the bone-like tissue that was deposited in the HAOB cell transplants. (**B**) The mRNA expression of *OCN, BSP* and *GAPDH* was measured by realtime polymerase chain reaction analysis using total RNA isolated from HAOB1-3 transplants and mock transplants.

BSP: Bone sialoprotein; HAOBs: Human alveolar bone osteoblasts; OCN: Osteocalcin; OPN: Osteopontin.

The first three populations obtained by sequential collagenase digestion did not exhibit osteogenic phenotypes and had low ALP activity and mineralization potential (data not shown). The subsequent fractions (4 – 8) showed osteogenic activity; therefore, we collected cells from fraction 5 and examined their ability to expand. HAOB1 (from a 66-year-old), HAOB2 (from a 52-year-old), HAOB3 (from a 53-year-old) and HAOB4 (from a 27-year-old) were successfully grown for > 30 PDs (**Figure 1A**). Interestingly, the growth ability of HAOB1-3 cultures, which were obtained from alveolar bones of middle-aged subjects, was comparable to that of HAOB4. To assess the safety of HAOBs as a cell source for regeneration therapy, we performed a karyotypic analysis (G banding and SKY; see the Materials and Methods section) using HAOB3 to assess the safety of the *ex vivo* expansion. SKY permits a detailed analysis of all complex markers and provides insight into their involvement in subsequent rearrangements. No genomic abnormalities were found in the HAOB3 culture at 16 PDs, as shown by G-banding and SKY analyses, and genomic stability was maintained in HAOBs at 35 PDs (**Figure 1B and C**). To investigate the bone-forming ability of HAOB3 *in vivo*, the cells were implanted into immunodeficient mice. Four weeks after implantation, HAOB1-4 generated bone tissue with osteocyte-like cells embedded on the hydroxyapatite beads (**Figure 2A**, upper panel). An immunohistochemical analysis revealed that the bone tissue was positive for anti-osteogenic marker antibodies, including OPN and OCN and that these transplants were detectable for the human-specific anti-vimentin antibody (**Figure 2A**). RT-PCR analysis confirmed that HAOB transplants strongly expressed human osteogenic genes, including *OCN* and *BSP* (**Figure 2B**). However, no bone tissue formation and mRNA expression of these genes were observed in transplants of β-TCP without human cells (**Figure 2B**). In light of these data, we used HAOB3 for the further characterization of HAOBs.

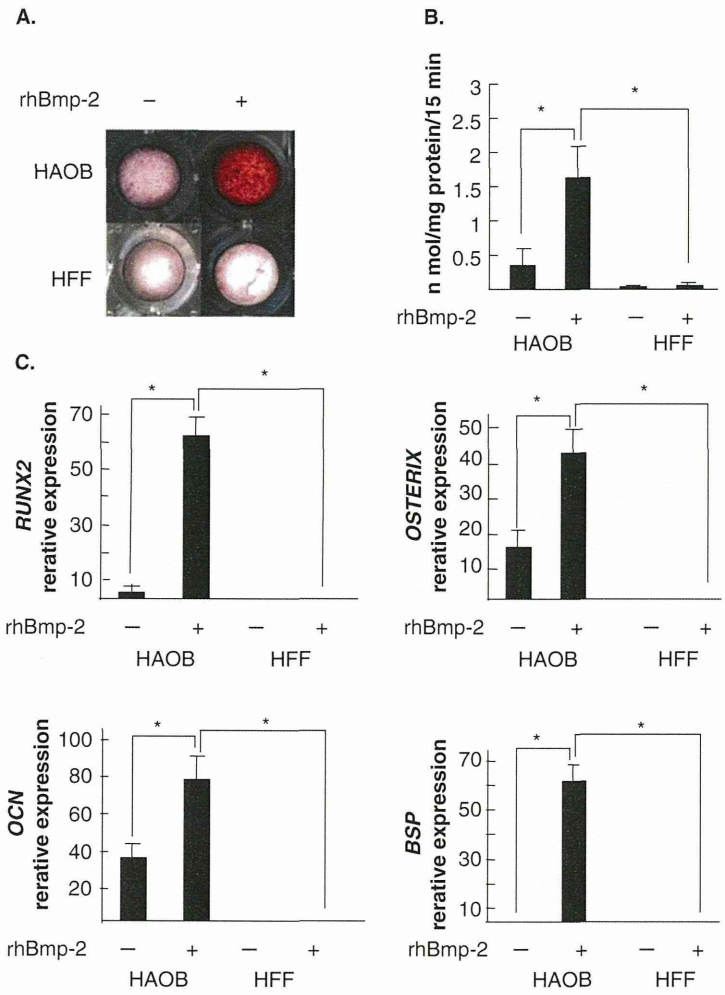

Figure 3. Osteogenic potential of HAOBs. HAOB3s were grown for 9 days in the medium with (+) or without (-) rhBMP-2 for analyzing alizarin red staining (**A**) and ALP activity (**B**). HFF was used as a control. (**C**) Total RNA from HAOB3 with (+) or without (-) treatment with rhBMP-2 was extracted and subjected to quantitative real-time PCR for the expression of *RUNX2, OSTERIX, OCN* and *BSP*. The levels of *β-ACTIN* transcript were used to normalize cDNA levels. The level of *β-ACTIN* was set to 100, and relative expression levels are shown. Data are presented as triplicates, and the mean ± s.d. are shown.

*$p > 0.05$.

ALP: Alkaline phosphatase; BSP: Bone sialoprotein; HAOBs: Human alveolar bone osteoblasts; HFF: Human foreskin fibroblast; OCN: Osteocalcin; rhBMP: Recombinant human bone morphogenic protein.

3.2 Osteogenic potential of HAOBs

To assess the osteogenic activity of HAOB3, the cells were treated with rhBMP-2 for 9 days. HAOB3 exhibited low ALP activity in an undifferentiated state, but the ALP activity and the ability to form mineralized nodules increased after treatment with rhBMP-2 (**Figure 3A and B**). RT-PCR analysis was performed to characterize the gene expression in HAOB3s by using primers for osteogenic genes, including *RUNX2, OSTERIX, OCN* and *BSP*. HAOB3 exhibited a modest expression of *OSTERIX* and *OCN* without treatment with rhBMP-2, but the expression of *RUNX2, OSTERIX, OCN* and *BSP* was clearly induced upon treatment with rhBMP-2 (**Figure 3C**). Because primary osteoblasts obtained from rodent calvaria were composed of a heterogeneous population, the authors investigated whether MSCs exist in HAOB3. A RT-PCR analysis indicated that the HAOBs did not express MSC marker genes, including CD73, CD90 and CD105 (**Figure 4A**). Although ALP activity is comparable to HAOB and MSC (**Figure 4C**), the HAOBs showed 10 times higher responsiveness to rhBMP-2 compared with MSC (**Figure 4B**), and a higher expression of osteogenic marker genes, including BSP, Runx2 and OCN, was detected (**Figure 4D**). The authors did not perform an adipogenic/chondrogenic differentiation assay because there was no expression of MSC marker genes in the HAOBs. Similar to MSC, the HOABs showed a higher osteogenic activity

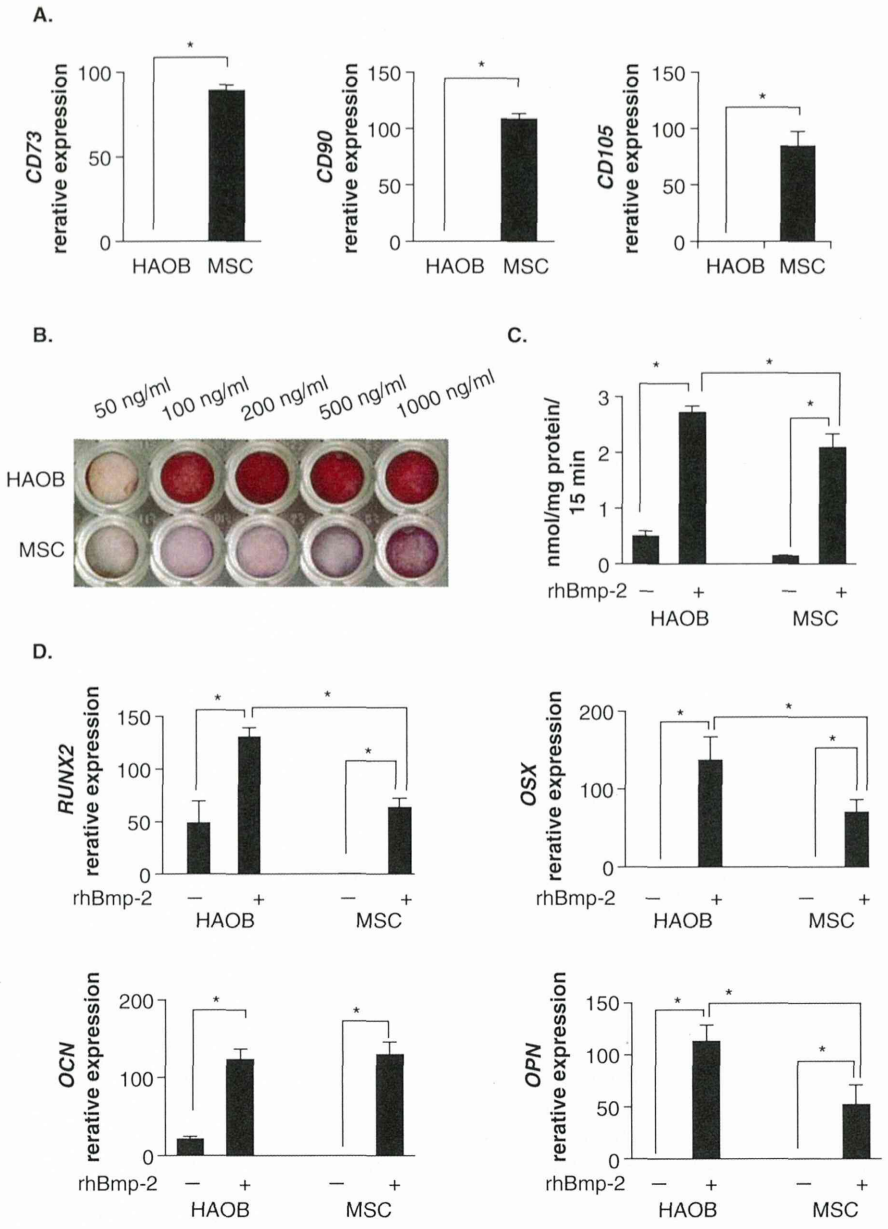

Figure 4. Comparison of the Osteogenic ability of HAOB and MSC. The mRNA expression levels of the undifferentiated markers, including *CD73, 90* and *105*, in the HAOBs and MSCs are shown (**A**). HAOB3s and MSCs were grown for 9 days in the medium with (+) or without (-) rhBMP2 at the indicated concentration to analyze the alizarin red staining (**B**) and ALPase activity. (**C**). The total RNA from HAOB3 and MSC with (+) or without (-) treatment with rhBMP2 was extracted and subjected to quantitative real-time PCR to express *RUNX2, OSTERIX, OCN* and *BSP*. The levels of *β-ACTIN* transcript were used to normalize cDNA levels. The level of *β-ACTIN* was set to 100, and the relative expression levels are shown. The data are presented as triplicates, and the mean ± s.d. are shown (**D**).

*p > 0.05.

ALP: Alkaline phosphatase; BSP: Bone sialoprotein; HAOBs: Human alveolar bone osteoblasts; MSC: Mesenchymal stem cells; OCN: Osteocalcin; rhBMP: Recombinant human bone morphogenic protein.

compared with that of human osteoblasts (Supplemental Figure 1). We next performed immunohistochemical analysis on HAOB3 using anti-OPN and anti-OCN antibodies to investigate the proportion of immature osteoblasts in the HAOB3 culture [31]. Confocal microscopy showed that most cells within the HAOB3 population were weakly positive OPN and OCN without treatment with rhBMP-2. In contrast, all cells within HAOB3 became strongly positive for

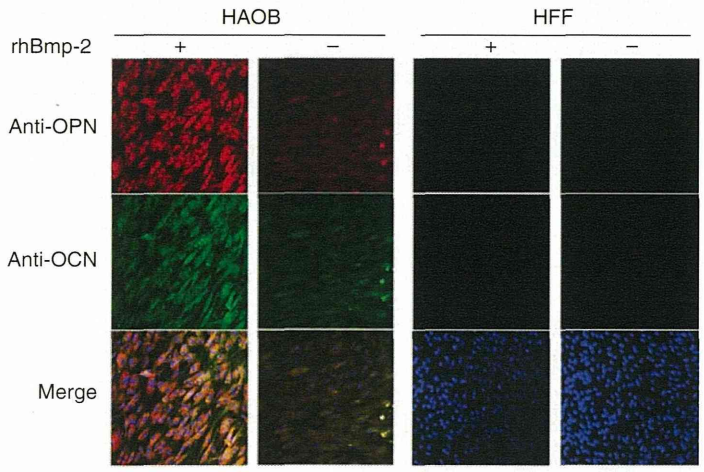

Figure 5. HAOBs are enriched in immature osteoblasts. HAOB3s and HFFs were grown on cover glass for 3 days in medium containing rhBMP-2, and immunohistochemical staining with anti-osteopontin polyclonal antibody and anti-osteocalcin monoclonal antibody was performed. The image is overlaid with DAPI staining. All of the cells within the HAOB3s were strongly positive for anti-OPN and anti-OCN antibodies upon treatment with rhBMP-2.

HAOBs: Human alveolar bone osteoblasts; HFF: Human foreskin fibroblast; OCN: Osteocalcin; OPN: Osteopontin; rhBMP: Recombinant human bone morphogenic protein.

OPN and OCN upon treatment with rhBMP-2. The superimposed image shows that the cells were double positive for these markers (**Figure 5**).

3.3 Identification of HAOB-specific genes

In general, the osteogenic activity of immature osteoblasts was decreased in association with increasing cell division. This effect may be due to dedifferentiation of immature osteoblasts. Because HAOB3 was able to grow for > 30 PDs, we next investigated whether HAOB3 undergoes dedifferentiation as PD increases. To address this question, HAOB3s were treated with rhBMP-2 at 6, 11, 16, 21, 24, 29, 32 and 35 PDs to evaluate their differentiation ability. Alizarin red staining revealed that the ability to form mineralized nodules was observed until 16 PDs; however, the activity was clearly downregulated after 21 PDs (**Figure 6A**, upper panel). Similar to the mineralization ability, ALP activity decreased after 29 PDs (**Figure 6A**, lower panel). RT-PCR analysis showed that the *OCN* expression level was maintained until 16 PDs; nevertheless, the expression was clearly downregulated after 21 PDs (**Figure 6B**). The expression of *RUNX2, OSTERIX* and *BSP* was also downregulated at 29 PDs compared with that at 6 PDs (**Figure 6C**).

Because the dedifferentiation of HAOB3s increased with successive PDs, the authors hypothesized that the genes specifically reduced in association of increasing PDs could serve as markers for HAOB3. To verify this possibility, total RNA was isolated from HAOB3 at 6, 11, 16, 21, 24, 29, 32 and 35 PDs, and the gene expression level was compared using Affymetrix HG-U133 Gene Chip analysis followed by an analysis with GeneSpringGX software. A PCA analysis revealed that a group of 3117 genes was annotated as downregulated in the HAOB3s as the PDs increased. **Table 1** shows the top downregulated genes in HAOB3, and we screened the genes that were highly expressed in the HAOB3s at 6 PDs but not at 35 PDs by RT-PCR analysis to identify the genes that are specifically expressed in HAOBs. From this screening, we identified *NEBL* as a candidate gene. RT-PCR analysis confirmed that *NEBL* was highly expressed in HAOB3 cultures at PD 6; however, its expression level was significantly downregulated at PD 35 (**Figure 6C**).

3.4 NEBL served as a marker for HAOBs

We next investigated whether *NEBL* is responsible for osteogenic differentiation by measuring the expression of this gene in HAOBs treated with rhBMP-2. The *NEBL* expression level increased with rhBMP-2 treatment, suggesting that it may be expressed during the osteogenic differentiation of HAOB (**Figure 7A**). To determine whether *NEBL* can be used as a marker for HAOB3s, the expression level of this gene was compared with those of osteogenic genes. As we expected, the expression of *NEBL* was apparently higher than that of *RUNX2, OSTERIX, OCN* and *BSP* (**Figure 7B**). These data suggest that *NEBL* can serve as a marker for undifferentiated HAOBs. To test this possibility, we next investigated whether *NEBL* was highly expressed in HAOBs. The expression level of this gene was compared with human mesenchymal cells, including MSC, normal human osteoblast (NHOst), human osteosarcoma cells (MG63) and HFFs. Higher expression of *NEBL* was observed in MSC as a positive control (**Figure 7D**), but intense expression of *NEBL* was observed in all of the HAOB cultures (HAOB1-4) at levels that were clearly higher than those in NHOst, MG63 and HFF (**Figure 7C**). To investigate the role of *NEBL* in regulating HAOB function, we evaluated whether *NEBL* induced by rhBMP-2 treatment affected the osteoblastic

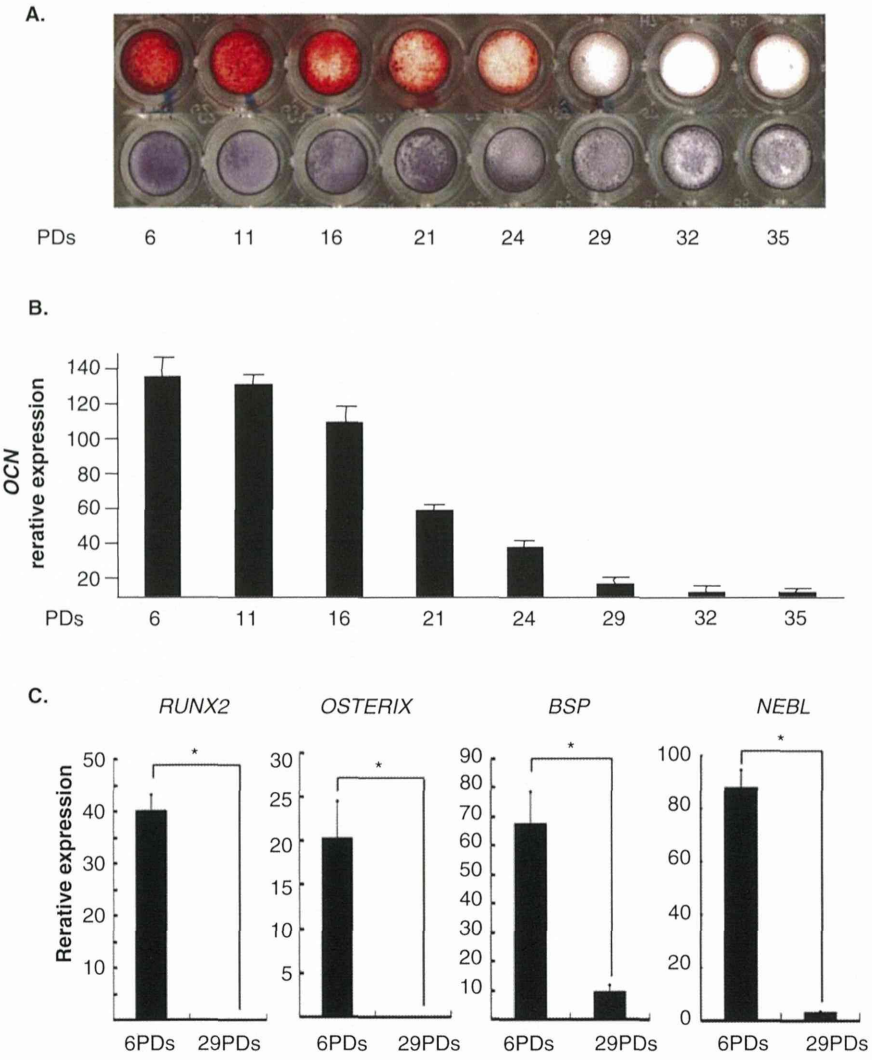

Figure 6. The decrease in the osteogenic potential of HAOBs was promoted with increasing cell division. (**A**) The osteogenic ability of HAOB3 with the indicated different PDs was investigated by alizarin red staining (upper panel) and ALP activity (lower panel). (**B**) The quantitative real-time PCR analysis of *OCN* expression is shown. Note that the dedifferentiation of HAOB3s was observed at 21 PDs. (**C**) Comparisons of the mRNA expression levels of *RUNX2, OSTERIX, BSP* and *NEBL* in HAOBs at 6 PD and 29 PD are shown.

*$p > 0.05$.

ALP: Alkaline phosphatase; BSP: Bone sialoprotein; HAOBs: Human alveolar bone osteoblasts; OCN: Osteocalcin.

differentiation of HAOBs. The knockdown of *NEBL* clearly inhibited mineralized nodule formation, ALP activity (**Figure 7E and F**) and expression of *RUNX2, OSX, OCN* and *BSP* after rhBMP-2 treatment (**Figure 7G**). However, no changes were observed in the HAOB cultures treated with control-siRNA treatment, further demonstrating that *NEBL* is involved in the osteoblastic differentiation of HAOB (**Figure 7D and E**).

4. Discussion

Because the demand for bone regeneration increases considerably in middle age, the effort to develop *ex vivo* expanded immature osteoblasts as a therapeutic agent for repairing critical bone defects is needed [32]. To date, juvenile immature osteoblasts have been shown to repair critical bone defects in animal models [14]. Nevertheless, efficacies of this type of cellular therapy using adult immature osteoblasts have yet to be developed due to the difficulty in culturing these cells. In the present study, we have outlined a method for the isolation and characterization of HAOBs from adult human immature osteoblasts from middle-aged donors. HAOBs were successfully expanded from the alveolar bone tissue of middle-aged donors and showed a high level of proliferative activity, different property of MSC and osteogenic ability upon treatment

Table 1. Genes specifically down regulated in association with increasing cell division are listed according to log change ratio.

Gene symbol	Gene product	Log change
ADH1B	Alcohol dehydrogenase IB (class I), β polypeptide	2.351
STMN2	Stathmin-like 2	2.221
GPX3	Glutathione peroxidase 3 (plasma)	1.859
NEBL	Nebulette	1.844
MGP	Matrix Gla protein	1.827
TRIB3	Chromosome 20 open-reading frame 97	1.804
SERPINA3	Serine proteinase inhibitor, clade A, member 3	1.795
PTGDS	Prostaglandin D2 synthase 21 kDa	1.782
APOE	Apolipoprotein E	1.769
PTGDS	Prostaglandin D2 synthase 21 kDa (brain)	1.754
MFAP4	Microfibrillar-associated protein 4	1.701
FBXO32	F-box only protein 32	1.694
TAC1	Tachykinin, precursor 1	1.681
KLF15	Kruppel-like factor 15	1.649
PPARGC1A	PPAR, γ, coactivator 1, α	1.647

with rhBMP-2 or implantation into immunodeficient mice. In addition, we suggest that expression level of *NEBL* is useful in assessing the osteoinductive potential of HAOB. These data demonstrate that HAOBs have properties of immature osteoblasts that indicate their potential to serve as a novel cell source for bone regeneration therapy.

The current challenge of bone regeneration therapy is to develop biomaterials that imitate the property of bone components, such as bioactive glass, including hydroxyapatite and β-calcium phosphate [17,33]. The osteoinductive properties of these materials have been improved by forming composites of biodegradable scaffolds, such as polylactide, chitosan and hyaluronic acid [34]. In addition, creating a device that incorporates immature osteoblasts in conjunction with biodegradable scaffolds has previously been reported to enhance bone regeneration ability [14]. MSCs have been used as a source of immature osteoblasts, and the autologous transplantation of MSCs on a biodegradable scaffold has been used in clinical study [35]. However, the number and proliferative capacity of human MSC derived from adult marrow aspirates have been shown to decrease, most likely due to an age-related decline in the number or growth capacity of immature osteoblasts [36,37]. Matsubara *et al.* reported that the success ratio of the expansion of bone marrow stromal cells from alveolar bone clearly decreased in patients > 40 years of age [25]. Previous findings have suggested that a reduction in the osteogenic and proliferative potential of osteogenic cells with aging is caused by changes in the secretion of IL-11 and IGF binding protein-3 or the responsiveness to basic fibroblast growth factor (bFGF) [38]. The ability of growth factors such as platelet-derived growth factor (PDGF) and bFGF to improve the proliferation of human osteoblast lineage cells has been studied [39,40]. In the present study, we show that HAOBs can be obtained from alveolar bone from patients > 60 years of age. Of the growth media tested, MF medium composed of 1% FCS containing various growth factors, including insulin, bFGF, PDGFs and IGF-1, was the most effective medium for the *ex vivo* expansion of HAOBs not only from middle-aged people but also from younger people. More importantly, HAOBs did not exhibit altered genomic stability or bone-forming ability upon transplantation into immunodeficient mice, suggesting that MF medium is suitable for the *ex vivo* expansion of HAOBs. Although a detailed description of the composition of MF medium is not available, our findings suggest that the identification of a specific combination of growth factors that induce the outgrowth of HAOBs may help to elucidate the role of the *ex vivo* expansion of cells from middle-aged humans.

Previous reports have shown that proliferative immature osteoblasts begin to express intermediate markers of osteogenic differentiation, such as OPN, and mature osteoblasts express OCN, which is a late marker of osteoblast differentiation [41,42]. The differentiation of immature osteoblasts is regulated by several cytokines, including BMP, transforming growth factors, Wnts and hedgehog [43-45]. Among these cytokines, BMP-2 strongly promotes osteoblast differentiation [44]. BMP-2 exhibited osteogenic activity by regulating the expression of osteoblast marker genes such as *ALP*, *OCN* and *BSP* [46]. BMP-2 also controls the expression of *RUNX2* and *OSX*, which are essential transcription factors for osteoblast differentiation [29,47,48]. These cells highly express *OPN* and *OCN* upon osteoblast differentiation by treatment with BMP-2. Previously, we demonstrated that immature osteoblasts could be isolated from BAOBs, which can differentiate into osteoblasts after treatment with osteogenic differentiation medium *in vitro* and generate bone tissue *in vivo*, suggesting that alveolar bone can serve as a reservoir for immature osteoblasts. In the present study, we demonstrated that most of the cells in HAOBs are weakly positive for OCN and OPN during proliferation and intensely induce the expression of these proteins after differentiation. Consistent with previous reports, the osteogenic differentiation of HAOBs was clearly induced upon treatment with rhBMP-2, as induced cells

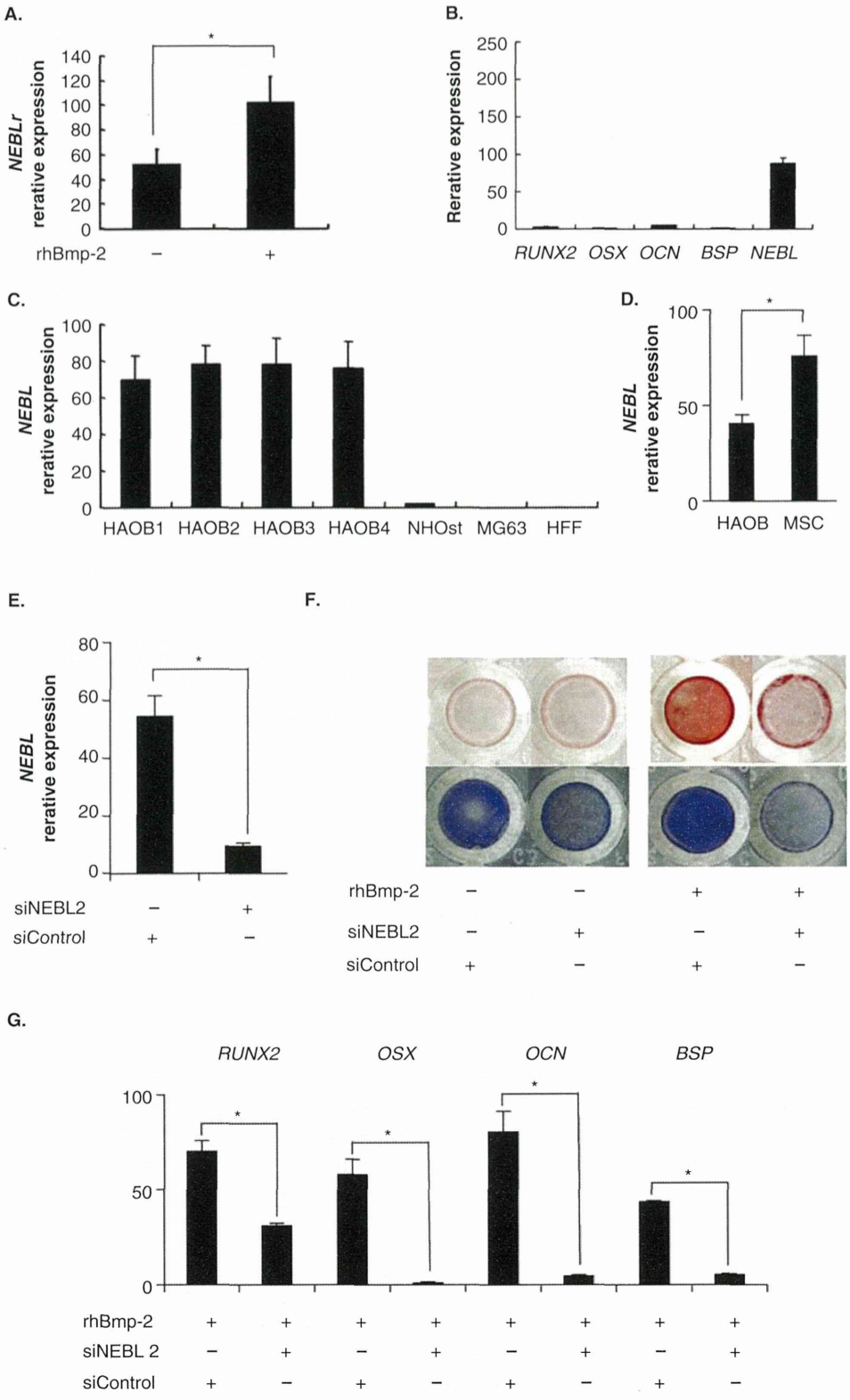

Figure 7. *NEBL* served as a marker of HAOBs with osteogenic potential. (**A**) Total RNA from HAOB3s with (+) or without (-) rhBMP-2 treatment was extracted and subjected to quantitative real-time PCR for the expression of *NEBL*. β-ACTIN transcript levels were used to normalize cDNA levels. (**B**) A comparison of the mRNA expression levels of *RUNX2, OSTERIX, OCN, BSP* and *NEBL* in HAOBs at 6 PD. (**C**) A comparison of the mRNA expression levels of *NEBL* in HAOBs and other osteoblastic cells. HFFs were used as a control. (**D**) The effect of *NEBL* siRNA on HAOB3 osteoblastic differentiation. HAOB3s treated with the indicated siRNAs for 72 h were grown for 9 days in medium with (+) or without (-) rhBMP-2 and analyzed by alizarin red staining (upper panel) and ALP activity (lower panel). (**E**) The effect of *NEBL* siRNA on mRNA expression levels. HAOB3s were treated with the indicated siRNAs for 72 h and treated with or without rhBMP-2, and osteogenic mRNA levels were measured by real-time PCR.

*$p > 0.05$.

ALP: Alkaline phosphatase; BSP: Bone sialoprotein; HAOBs: Human alveolar bone osteoblasts; HFF: Human foreskin fibroblast; OCN: Osteocalcin; rhBMP: Recombinant human bone morphogenic protein.

exhibited ALP activity, mineralized nodule formation and the expression of bone marker genes, including *RUNX2*, *OSX*, *OCN* and *BSP*. These findings indicate that HAOBs are enriched in immature osteoblasts that can differentiate in response to treatment with BMP-2.

Cell-based bone tissue engineering requires the expansion and seeding of immature osteoblasts onto a scaffold; however, dedifferentiation occurred with increasing cell division during cellular senescence [7]. To avoid these problems, a functional marker for the assessment of the differentiation ability is required to establish a proper *ex vivo* expansion system. In this study, we suggest the potential use of NEBL as a quality marker in assessments of the osteoinductive ability of HAOBs. NEBL which belongs to Nebulin, an actin-binding protein, is a member of a cytoskeletal protein family that is a component of a variety of cytoskeletal structures [49-51]. It encodes a sarcomeric Z-disk protein, contributes to the generation of muscle force via its interaction with actin and the cardiac tropomyosin/troponin complex and participates in the force transmission of the cardiac myofibril via the Z-disk assembly [52]. Humans carrying NEBL mutations exhibit dilated cardiomyopathy, a cardiac disease characterized by the dilation of the left ventricular cavity and systolic dysfunction [53]. Transcriptome profiles that are associated with osteogenic, chondrogenic and adipogenic differentiations from human MSC indicate that the expression of NEBL is increased during the differentiation of all three lineages [54]. Previous studies have indicated that actin cytoskeletal rearrangement participates in MSC lineage selection, preventing adipogenesis and stimulating osteogenic differentiation through the generation of a stiffer cytoskeleton [55]. These findings indicate that NEBL may play a role in the maintenance and differentiation of immature osteoblasts via the regulation of cytoskeletal rearrangement. Recently, a defined serum-free medium consisting of the minimum essential components has been developed as a safety culture system that avoids components of fetal bovine serum for clinical application [56]. To develop such a cell culture system, functional markers that assess the osteogenic ability of HAOBs, such as *NEBL*, could be used to estimate the efficacy of the media. An index of NEBL expression level could also contribute to the exploitation of the novel *ex vivo* expansion of HAOBs that maintain their osteogenic ability.

5. Conclusion

In conclusion, this study demonstrates the establishment of an HAOB culture system that possesses an immature osteoblast phenotype and robust osteogenic activity. Further studies on growth factors that induce HAOB cell expansion or appropriate biodegradable scaffolds for bone regeneration are needed. This approach will facilitate regeneration therapy for treating chronic inflammatory disease associated with large bone defects, such as periodontal disease.

Acknowledgements

We greatly thank Riko Nishimura, Kenji Hata, Masamitsu Oshima and Takashi Tsuji for their valuable advice and discussions during the course of this work. We also acknowledge Olympus Co. for kindly donating the OSferion.

Declaration of interest

This work was supported by the Ministry of Health Labour and Welfare through a Health Labour Sciences Research Grant for Comprehensive Research on Aging and Health to M Saito. The authors have no other relevant affiliations or financial involvement with any organization or entity with a financial interest in or financial conflict with the subject matter or materials discussed in the manuscript apart from those disclosed.

Bibliography

Papers of special note have been highlighted as either of interest (•) or of considerable interest (••) to readers.

1. Gruber R, Koch H, Doll BA, et al. Fracture healing in the elderly patient. Exp Gerontol 2006;41(11):1080-93
2. Mistry AS, Mikos AG. Tissue engineering strategies for bone regeneration. Adv Biochem Eng Biotechnol 2005;94:1-22
3. Lin CY, Schek RM, Mistry AS, et al. Functional bone engineering using ex vivo gene therapy and topology-optimized, biodegradable polymer composite scaffolds. Tissue Eng 2005;11(9-10):1589-98
4. Bauer TW, Muschler GF. Bone graft materials. An overview of the basic science. Clin Orthop Relat Res 2000(371):10-27
5. Zhang ZY, Teoh SH, Chong MS, et al. Neo-vascularization and bone formation mediated by fetal mesenchymal stem cell tissue-engineered bone grafts in critical-size femoral defects. Biomaterials 2010;31(4):608-20
6. Liu J, Liu C, Sun B, et al. Differentiation of rabbit bone mesenchymal stem cells into endothelial cells in vitro and promotion of defective bone regeneration in vivo. Cell Biochem Biophys 2014;68(3):479-87
7. Zhou S, Greenberger JS, Epperly MW, et al. Age-related intrinsic changes in human bone-marrow-derived mesenchymal stem cells and their differentiation to osteoblasts. Aging Cell 2008;7(3):335-43
- **This article showed age-dependent dedifferentiation mechanisms were interfered human mesenchymal stem cells potential including proliferation and differentiation.**
8. Phillips JE, Gersbach CA, Garcia AJ. Virus-based gene therapy strategies for bone regeneration. Biomaterials 2007;28(2):211-29
9. Chang J, Sonoyama W, Wang Z, et al. Noncanonical Wnt-4 signaling enhances bone regeneration of mesenchymal stem

cells in craniofacial defects through activation of p38 MAPK. J Biol Chem 2007;282(42):30938-48

10. Peng H, Wright V, Usas A, et al. Synergistic enhancement of bone formation and healing by stem cell-expressed VEGF and bone morphogenetic protein-4. J Clin Invest 2002;110(6):751-9
11. Petite H, Viateau V, Bensaid W, et al. Tissue-engineered bone regeneration. Nat Biotechnol 2000;18(9):959-63
12. Yamada Y, Boo JS, Ozawa R, et al. Bone regeneration following injection of mesenchymal stem cells and fibrin glue with a biodegradable scaffold. J Craniomaxillofac Surg 2003;31(1):27-33
13. Oryan A, Alidadi S, Moshiri A, Maffulli N. Bone regenerative medicine: classic options, novel strategies, and future directions. J Orthop Surg Res 2014;9(1):18
14. Cowan CM, Shi YY, Aalami OO, et al. Adipose-derived adult stromal cells heal critical-size mouse calvarial defects. Nat Biotechnol 2004;22(5):560-7

• **This article showed immature osteoblast transplantation is capable of regenerating critical size of bone defect.**

15. Tsuchiya K, Mori T, Chen G, et al. Custom-shaping system for bone regeneration by seeding marrow stromal cells onto a web-like biodegradable hybrid sheet. Cell Tissue Res 2004;316(2):141-53
16. Komori T. Regulation of osteoblast differentiation by transcription factors. J Cell Biochem 2006;99(5):1233-9
17. Mravic M, Peault B, James AW. Current trends in bone tissue engineering. Biomed Res Int 2014;2014:865270

• **This review focused on culture techniques combined with biodegradable scaffolds as a reliable therapeutic strategy for bone regeneration.**

18. Guang LG, Boskey AL, Zhu W. Age-related CXC chemokine receptor-4-deficiency impairs osteogenic differentiation potency of mouse bone marrow mesenchymal stromal stem cells. Int J Biochem Cell Biol 2013;45(8):1813-20
19. Perinpanayagam H, Martin T, Mithal V, et al. Alveolar bone osteoblast differentiation and Runx2/Cbfa1 expression. Arch Oral Biol 2006;51(5):406-15
20. Palmer RM, Lumsden AG. Development of periodontal ligament and alveolar bone in homografted recombinations of enamel organs and papillary, pulpal and follicular mesenchyme in the mouse. Arch Oral Biol 1987;32(4):281-9
21. Melsen B. Biological reaction of alveolar bone to orthodontic tooth movement. Angle Orthod 1999;69(2):151-8
22. Xiao Y, Qian H, Young WG, Bartold PM. Tissue engineering for bone regeneration using differentiated alveolar bone cells in collagen scaffolds. Tissue Eng 2003;9(6):1167-77
23. Choi BH, Zhu SJ, Kim BY, et al. Effect of platelet-rich plasma (PRP) concentration on the viability and proliferation of alveolar bone cells: an in vitro study. Int J Oral Maxillofac Surg 2005;34(4):420-4
24. Zhu SJ, Choi BH, Huh JY, et al. A comparative qualitative histological analysis of tissue-engineered bone using bone marrow mesenchymal stem cells, alveolar bone cells, and periosteal cells. Oral Surg Oral Med Oral Pathol Oral Radiol Endod 2006;101(2):164-9
25. Matsubara T, Suardita K, Ishii M, et al. Alveolar bone marrow as a cell source for regenerative medicine: differences between alveolar and iliac bone marrow stromal cells. J Bone Miner Res 2005;20(3):399-409
26. Greenwood SK, Hill RB, Sun JT, et al. Population doubling: a simple and more accurate estimation of cell growth suppression in the in vitro assay for chromosomal aberrations that reduces irrelevant positive results. Environ Mol Mutagen 2004;43(1):36-44

•• **This article shows bone derived bone marrow stromal cells (BMSC) obtained from alveolar bone possessed osteogenic ability and their characters are resembled those of iliac BMSC.**

27. Handa K, Saito M, Yamauchi M, et al. Cementum matrix formation in vivo by cultured dental follicle cells. Bone 2002;31(5):606-11

•• **This article shows that bovine alveolar bone osteoblasts isolated from adult alveolar bone possessed high osteogenic ability upon implantation into immunodeficiency mice.**

28. Schrock E, du Manoir S, Veldman T, et al. Multicolor spectral karyotyping of human chromosomes. Science 1996;273(5274):494-7
29. Matsubara T, Kida K, Yamaguchi A, et al. BMP2 regulates Osterix through Msx2 and Runx2 during osteoblast differentiation. J Biol Chem 2008;283(43):29119-25
30. Kami D, Shiojima I, Makino H, et al. Gremlin enhances the determined path to cardiomyogenesis. PLoS One 2008;3(6):e2407
31. Mansukhani A, Bellosta P, Sahni M, Basilico C. Signaling by fibroblast growth factors (FGF) and fibroblast growth factor receptor 2 (FGFR2)-activating mutations blocks mineralization and induces apoptosis in osteoblasts. J Cell Biol 2000;149(6):1297-308
32. Maegawa N, Kawamura K, Hirose M, et al. Enhancement of osteoblastic differentiation of mesenchymal stromal cells cultured by selective combination of bone morphogenetic protein-2 (BMP-2) and fibroblast growth factor-2 (FGF-2). J Tissue Eng Regen Med 2007;1(4):306-13
33. Caplan AI. Adult mesenchymal stem cells for tissue engineering versus regenerative medicine. J Cell Physiol 2007;213(2):341-7
34. Burg KJ, Porter S, Kellam JF. Biomaterial developments for bone tissue engineering. Biomaterials 2000;21(23):2347-59
35. Bianco P, Robey PG. Stem cells in tissue engineering. Nature 2001;414(6859):118-21
36. Stenderup K, Justesen J, Eriksen EF, et al. Number and proliferative capacity of osteogenic stem cells are maintained during aging and in patients with osteoporosis. J Bone Miner Res 2001;16(6):1120-9
37. Oreffo RO, Bord S, Triffitt JT. Skeletal progenitor cells and ageing human populations. Clin Sci (Lond) 1998;94(5):549-55
38. Cowan CM, Quarto N, Warren SM, et al. Age-related changes in the biomolecular mechanisms of calvarial osteoblast biology affect fibroblast growth

factor-2 signaling and osteogenesis. J Biol Chem 2003;278(34):32005-13

•• **In this study, author investigated cellular and molecular differences between primary osteoblasts derived from juvenile and adult rat calvaria.**

39. Li P, Bai Y, Yin G, et al. Synergistic and sequential effects of BMP-2, bFGF and VEGF on osteogenic differentiation of rat osteoblasts. J Bone Miner Metab 2013. [Epub ahead of print]
40. Caverzasio J, Biver E, Thouverey C. Predominant role of PDGF receptor transactivation in Wnt3a-induced osteoblastic cell proliferation. J Bone Miner Res 2013;28(2):260-70
41. zur Nieden NI, Kempka G, Ahr HJ. In vitro differentiation of embryonic stem cells into mineralized osteoblasts. Differentiation 2003;71(1):18-27
42. Candeliere GA, Liu F, Aubin JE. Individual osteoblasts in the developing calvaria express different gene repertoires. Bone 2001;28(4):351-61
43. Baron R, Rawadi G. Wnt signaling and the regulation of bone mass. Curr Osteoporos Rep 2007;5(2):73-80
44. Cohen MM Jr. The new bone biology: pathologic, molecular, and clinical correlates. Am J Med Genet A 2006;140(23):2646-706
45. Hu H, Hilton MJ, Tu X, et al. Sequential roles of Hedgehog and Wnt signaling in osteoblast development. Development 2005;132(1):49-60
46. Chen D, Zhao M, Mundy GR. Bone morphogenetic proteins. Growth Factors 2004;22(4):233-41
47. Komori T, Yagi H, Nomura S, et al. Targeted disruption of Cbfa1 results in a complete lack of bone formation owing to maturational arrest of osteoblasts. Cell 1997;89(5):755-64
48. Nakashima K, Zhou X, Kunkel G, et al. The novel zinc finger-containing transcription factor osterix is required for osteoblast differentiation and bone formation. Cell 2002;108(1):17-29
49. Moncman CL, Wang K. Nebulette: a 107 kD nebulin-like protein in cardiac muscle. Cell Motil Cytoskeleton 1995;32(3):205-25
50. Pappas CT, Bliss KT, Zieseniss A, Gregorio CC. The Nebulin family: an actin support group. Trends Cell Biol 2011;21(1):29-37
51. Lee EJ, De Winter JM, Buck D, et al. Fast skeletal muscle troponin activation increases force of mouse fast skeletal muscle and ameliorates weakness due to nebulin-deficiency. PLoS One 2013;8(2):e55861
52. Bang ML, Mudry RE, McElhinny AS, et al. Myopalladin, a novel 145-kilodalton sarcomeric protein with multiple roles in Z-disc and I-band protein assemblies. J Cell Biol 2001;153(2):413-27
53. Purevjav E, Varela J, Morgado M, et al. Nebulette mutations are associated with dilated cardiomyopathy and endocardial fibroelastosis. J Am Coll Cardiol 2010;56(18):1493-502

•• **This article shows the nebulette that belongs to nebulin family is involved in assembly of cytoskeletal structures, and expressed tissue-specific manner.**

54. Eslaminejad MB, Yazdi PE. Mesenchymal stem cells: in vitro differentiation among bone and cartilage cell lineages. Yakhteh Med J 2007;9(3):158-69
55. Sen B, Xie Z, Case N, et al. mTORC2 regulates mechanically induced cytoskeletal reorganization and lineage selection in marrow-derived mesenchymal stem cells. J Bone Miner Res 2014;29(1):78-89

• **These results indicate the importance of actin cytosketal arrangement in regulation of osteogenic differentiation.**

56. Solchaga LA, Penick K, Goldberg VM, et al. Fibroblast growth factor-2 enhances proliferation and delays loss of chondrogenic potential in human adult bone-marrow-derived mesenchymal stem cells. Tissue Eng Part A 2010;16(3):1009-19

Affiliation

Makoto Aino[1], Eisaku Nishida[1], Yoshiyasu Fujieda[7], Ai Orimoto[2], Akio Mitani[1], Toshihide Noguchi[1], Hatsune Makino[4], Shinya Murakami[3], Akihiro Umezawa[5], Toshiyuki Yoneda[6] & Masahiro Saito[†8] DDS PhD
[†]Author for correspondence
[1]Aichi-gakuin University, School of Dentistry, Department of Periodontology, Nagoya, Aichi, Japan
[2]University Graduate School of Dentistry, Department of Restorative Dentistry, Tohoku Sendai, Miyagi, Japan
[3]Osaka University Graduate School of Dentistry, Department of Periodontology and Oral Pathology, Suita, Osaka, Japan
[4]The University of Tokyo, Institute of Molecular and Cellular Biosciences, Cardiovascular Regeneration, Tokyo, Japan
[5]National Research Institute for Child and Health Development, Department of Reproductive Biology and Pathology, Tokyo, Japan
[6]Indiana University School of Medicine, Division Hematology/Oncology, Indianapolis, IN, USA
[7]Tokyo University of Science, Graduate School of Industrial Science and Technology, Department of Biological Science and Technology, Noda, 278-8510, Japan
[8]Tohoku University Graduate School of Dentistry, Division of Operative Dentistry, Department of Restorative Dentistry, 4-1 Seiryo-machi, Aoba-ku, 980-8575 Sendai, Japan
Tel: +81 22 717 8340;
Fax: +81 22 717 8343;
E-mail: mssaito@dent.tohoku.ac.jp

Supplementary materials available online

Supplemental Figure 1.

Journal of
PERIODONTAL RESEARCH

J Periodont Res 2014

JOURNAL OF PERIODONTAL RESEARCH
doi:10.1111/jre.12202

Effects of the proteasome inhibitor, bortezomib, on cytodifferentiation and mineralization of periodontal ligament cells

J. Kitagaki[1,2]*, S. Miyauchi[1]*
C. J Xie[1,3], M. Yamashita[1]
S. Yamada[1], M. Kitamura[1]
S. Murakami[1]

[1]Department of Periodontology, Division of Oral Biology and Disease Control, Osaka University Graduate School of Dentistry, Suita, Osaka, Japan, [2]Challenge to Intractable Oral Diseases, Center for Translational Dental Research, Osaka University Dental Hospital, Suita, Osaka, Japan and [3]Department of Periodontology, Stomatology Hospital of Guangdong Province, Southern Medical University, Guangzhou, China

Kitagaki J, Miyauchi S, Xie CJ, Yamashita M, Yamada S, Kitamura M, Murakami S. Effects of the proteasome inhibitor, bortezomib, on cytodifferentiation and mineralization of periodontal ligament cells. J Periodont Res 2014; doi: 10.1111/jre.12202. © 2014 John Wiley & Sons A/S. Published by John Wiley & Sons Ltd

Background and Objective: The proteasome inhibitor, bortezomib, is known to induce osteoblastic differentiation in a number of cell lines, such as mesenchymal stem cells and osteoblastic precursor cells. As periodontal ligament (PDL) cells are multipotent, we examined whether bortezomib may induce the differentiation of PDL cells into hard-tissue-forming cells.

Material and Methods: A mouse PDL clone cell line, MPDL22 cells, was cultured in mineralization medium in the presence or absence of bortezomib. Expression of calcification-related genes and calcified-nodule formation were evaluated by real-time PCR and Alizarin Red staining, respectively.

Results: Bortezomib increased the expression of calcification-related mRNAs, such as tissue nonspecific alkaline phosphatase isoenzyme (*ALPase*), bone sialoprotein (*Bsp*), runt-related transcription factor 2 (*Runx2*) and osteopontin, and calcified-nodule formation in MPDL22 cells. These effects were induced, in part, by increasing the cytosolic accumulation and nuclear translocation of β-catenin, leading to an increase in expression of bone morphogenetic protein (*Bmp*)-*2*, -*4* and -*6* mRNAs. In addition, bortezomib enhanced BMP-2-induced expression of *Bsp* and osteopontin mRNAs and increased calcified-nodule formation in MPDL22 cells.

Conclusion: Bortezomib induced cytodifferentiation and mineralization of PDL cells by enhancing the accumulation of β-catenin within the cytosol and the nucleus and increasing the expression of *Bmp-2, -4* and *-6* mRNAs. Moreover, bortezomib enhanced the BMP-2-induced cytodifferentiation and mineralization of PDL cells, suggesting that bortezomib may be efficacious for use in periodontal regeneration therapy.

Shinya Murakami, DDS, PhD, Department of Periodontology, Division of Oral Biology and Disease Control, Osaka University Graduate School of Dentistry, 1-8 Yamadaoka, Suita, Osaka 565-0871, Japan
Tel: +81 6 6879 2930
Fax: +81 6 6879 2934
e-mail: ipshinya@dent.osaka-u.ac.jp

*These authors contributed equally to this work.

Key words: bortezomib; cytodifferentiation; mineralization; periodontal ligament

Accepted for publication May 01, 2014

The periodontal ligament (PDL), which is located between the cementum covering root dentin and the alveolar bone, is a unique connective tissue that supports the teeth (1). Importantly, the PDL contains multipotential mesenchymal stem cells and progenitor cells that can differentiate into mineralized tissue-forming cells, including cementoblasts and osteoblasts (2). Consequently, the PDL has an important role to play not only in the

maintenance of periodontal tissues, but also in bone remodeling, repair and tissue regeneration. Thus, improving and/or enhancing the biological potential of PDL cells is clinically very important to stimulate the regeneration of periodontal tissue that has been destroyed by periodontitis.

A number of studies have demonstrated that protein degradation by the ubiquitin proteasome system controls numerous signaling pathways and induces a wide variety of biological effects, such as regulation of the cell cycle, apoptosis, proliferation and differentiation (3). Bortezomib (Velcade®) is a reversible inhibitor of the chymotrypsin-like activity of the ubiquitin proteasome system and is highly effective in multiple myeloma, where it inhibits nuclear factor-κB activation and interleukin-6-mediated cell growth (4). Because of these effects, bortezomib was approved by the US Food and Drug Administration, in 2005, for the treatment of patients with multiple myeloma. Interestingly, bortezomib not only increases bone mass in a variety of bone defects *in vivo*, but also induces mesenchymal stem cells to undergo preferentially osteoblastic differentiation *in vitro* (5–9).

Because the PDL contains multipotential mesenchymal stem cells, we hypothesized that bortezomib may regulate the osteoblastic differentiation of PDL cells. In the present study, we demonstrate that bortezomib stimulates cytodifferentiation and mineralization of a mouse PDL clone cell line, MPDL22 cells, as assessed by real-time PCR and Alizarin Red staining, respectively. These effects were achieved partially through an increase in the cytosolic accumulation and nuclear translocation of β-catenin and the expression of bone morphogenetic protein *(Bmp)-2*, *-4* and *-6* mRNAs. We also found that culturing cells with bortezomib enhanced the BMP-2-induced cytodifferentiation and mineralization of MPDL22 cells. These data indicate that bortezomib may be a promising compound for the regeneration of periodontal tissues destroyed by periodontal disease.

Material and methods

Reagents and cell lines

The proteasome inhibitor, bortezomib, and anti-β-catenin IgG were purchased from Cell Signaling Technology (Danvers, MA, USA). Recombinant human BMP-2 was purchased from R&D Systems (Minneapolis, MN, USA). Anti-β-actin IgG was purchased from Sigma (St Louis, MO, USA). Anti-ubiquitin IgG was purchased from Santa Cruz Biotechnology (Santa Cruz, CA, USA). Human recombinant fibroblast growth factor-2 was provided by Kaken Pharmaceutical Co., Ltd. (Tokyo, Japan). A mouse PDL clone cell line, MPDL22 cells, was isolated and cultured as described previously (10). Briefly, MPDL22 cells were maintained in a standard medium of α-MEM (Nikken, Kyoto, Japan) supplemented with both 10% fetal calf serum and 100 ng/mL of fibroblast growth factor-2. When the cells became confluent, we removed fibroblast growth factor-2 from the culture medium and replaced it with mineralization medium (α-MEM supplemented with 10% fetal calf serum, 5 mM β-glycerophosphate and 50 μg/mL of L-ascorbic acid). Human PDL (HPDL) cells were purchased from ScienCell Research Laboratories (Carlsbad, CA, USA) and were maintained in a standard medium of α-MEM supplemented with 10% fetal calf serum. To differentiate HPDL cells into hard-tissue-forming cells, we replaced growth medium with mineralization medium.

Immunoblotting

Cell lysates were prepared as described previously (11–13). For the preparation of total protein, cells were lysed with RIPA buffer [50 mM Tris (pH 7.5), 150 mM NaCl, 1% Nonidet P-40, 0.5% sodium deoxycholate, 0.1% SDS and Complete Mini (Roche, Mannheim, Germany)] and centrifuged at 13,000 *g* for 20 min. For the preparation of nuclear extract, cells were lysed with Buffer A [10 mM HEPES-KOH (pH 7.8), 10 mM KCl, 0.1% Nonidet P-40, 0.1 mM EDTA (pH 8.0) and Complete Mini] and centrifuged at 2,500 *g* for 1 min. The resultant pellet was then lysed with Buffer C [50 mM HEPES-KOH (pH 7.8), 420 mM KCl, 0.1 mM EDTA (pH 8.0), 5 mM $MgCl_2$, 2% glycerol and Complete Mini], incubated on ice for 30 min and centrifuged at 20,000 *g* for 15 min. For analysis of the accumulation of β-catenin in the cytosol, cells were lysed with TBS [10 mM Tris–HCl (pH 7.4), 140 mM NaCl and Complete Mini], passaged 30 times through a 22-gauge needle and then centrifuged at 1,100 *g* for 5 min. The resultant supernatant was centrifuged at 100,000 *g* for 90 min. Equal amounts of cell lysates were resolved by SDS-PAGE, transferred to poly(vinylidene difluoride) membranes (Millipore, Kansas City, MO, USA), incubated with specific primary antibodies and horseradish peroxidase-conjugated second antibodies (Thermo Fisher Scientific, Waltham, MA, USA) and visualized with chemiluminescence agents (Pierce, Rockford, IL, USA), according to the manufacturer's instructions.

Trypan Blue exclusion

Cell viability was analyzed using Trypan Blue staining and subsequent microscopy. Equal volumes of culture medium-suspended cells and Trypan Blue reagent (Wako, Osaka, Japan) were mixed for 1 min. Analysis by microscopy showed that nonviable cells were stained with Trypan Blue reagent, whereas viable cells excluded the stain.

WST-1 assay

The number of metabolically active cells was analyzed using a nonradioactive colorimetric assay, the WST-1 assay, according to the manufacturer's instructions (Roche, Basel, Switzerland). Briefly, MPDL22 cells were seeded into 96-well plates (1×10^4 cells/well) and incubated with bortezomib for 24 h in 100 μL of complete medium. Ten microliters of WST-1 reagent was then added to each well. Following incubation for 60 min, the OD 450/630 nm was measured using a microplate reader (Bio-Rad, Hercules, CA, USA). The results were expressed as a percentage

of measurement as compared with the vehicle control wells.

Alizarin Red staining

The histochemical staining of calcified-nodule formation was performed using Alizarin Red stain (14). Briefly, the cell layers were washed with phosphate-buffered saline and then fixed with dehydrated ethanol for 10 min. After fixation, the cell layers were stained with 1% Alizarin Red S in 0.1% NH_4OH (pH 6.3–6.5) for 5 min and then washed with water. The density of calcified nodules was analyzed using the WinRoof software, version 5.6 (Mitani, Fukui, Japan).

ELISA

BMP-2 protein levels in the culture supernatant were measured by ELISA, according to the manufacturer's instructions (R&D Systems).

Real-time PCR analysis

Total RNA from MPDL22 and HPDL cells was isolated using RNA bee (Tel-Test Inc., Friendswood, TX, USA) and reverse transcribed using a High Capacity RNA-to-cDNA Kit (Applied Biosystems, Carlsbad, CA, USA), according to the manufacturer's instructions. The resultant cDNA was then mixed with Power PCR SYBR Master Mix (Applied Biosystems) and gene-specific PCR primers. The primer sequences for the real-time PCR were as follows: mouse glyceraldehyde-3-phosphate dehydrogenase (*Gapdh*), (forward) 5′-TGT GTC CGT CGT GGA TCT GA-3′ and (reverse) 5′-TTG CTG TTG AAG TCG CAG GAG-3′; mouse tissue nonspecific alkaline phosphatase isoenzyme (*ALPase*), (forward) 5′-ACA CCT TGA CTG TGG TTA CTG CTG A-3′ and (reverse) 5′-CCT TGT AGC CAG GCC CGT TA-3′; mouse bone sialoprotein (*Bsp*), (forward) 5′-TGG AGA CTG CGA TAG TTC CGA AG-3′ and (reverse) 5′-CGT AGC TAG CTG TTA CAC CCG AGA G-3′; mouse osteopontin, (forward) 5′-TAC GAC CAT GAG ATT GGC AGT GA-3′ and (reverse) 5′-TAT AGG ATC TGG GTG CAG GCT GTA A-3′; mouse runt-related transcription factor 2 (*Runx2*), (forward) 5′-CAC TGG CGG TGC AAC AAG A-3′ and (reverse) 5′-TTT CAT AAC AGC GGA GGC ATT TC-3′; mouse *Bmp2*, (forward) 5′-TGA CTG GAT CGT GGC ACC TC-3′ and (reverse) 5′-CAG AGT CTG CAC TAT GGC ATG GTT A-3′; mouse *Bmp4*, (forward) 5′-TTT GTT CAA GAT TGG CTC CCA AG -3′ and (reverse) 5′-AAA CGA CCA TCA GCA TTC GGT TA-3′; mouse *Bmp6*, (forward) 5′-AGT CTT GCA GGA GCA TCA GCA C-3′ and (reverse) 5′-GTG TCA CCA CCC ACA GAT TGC TA-3′; human hypoxanthine-guanine phosphoribosyltransferase (*HPRT*), (forward) 5′-GGC AGT ATA ATC CAA AGA TGG TCA A-3′ and (reverse) 5′-GTC AAG GGC ATA TCC TAC AAC AAA C-3′; human *BSP*, (forward) 5′-GGC CAC GAT ATT ATC TTT ACA AGC A-3′ and (reverse) 5′-TCA GCC TCA GAG TCT TCA TCT TCA-3′; and human osteopontin, (forward) 5′-GAT GAA TCT GAT GAA CTG GTC ACT G-3′ and (reverse) 5′-GGT GAT GTC CTC GTC TGT AGC A-3′. Real-time PCR reactions were carried out using a 7300 Fast Real-Time RT-PCR system (Applied Biosystems), according to the manufacturer's instructions. After an initial denaturation at 95°C for 15 min, 40 cycles, each consisting of denaturation at 94°C for 15 s, annealing at 60°C for 30 s and elongation at 72°C for 30 s, were performed.

Statistical analysis

The results were analyzed for statistical significance using the Student's *t*-test. The differences between two means were considered significant at p values less than 0.05.

Results

Effects of bortezomib on the proliferation, viability and proteasome activity of MPLD22 cells

To elucidate the influence of bortezomib on the various functions of PDL cells, we first analyzed the effects of bortezomib on the proliferation and viability of MPDL22 cells. MPDL22 cells were treated with bortezomib, then cell proliferation and viability were assessed using the WST-1 assay and Trypan Blue exclusion, respectively. Because bortezomib was dissolved in dimethylsulfoxide in this study, dimethylsulfoxide alone was utilized as the control. Bortezomib did not affect the proliferation or viability of MPDL22 cells at doses of 1–10 nM (Fig. 1A and 1B).

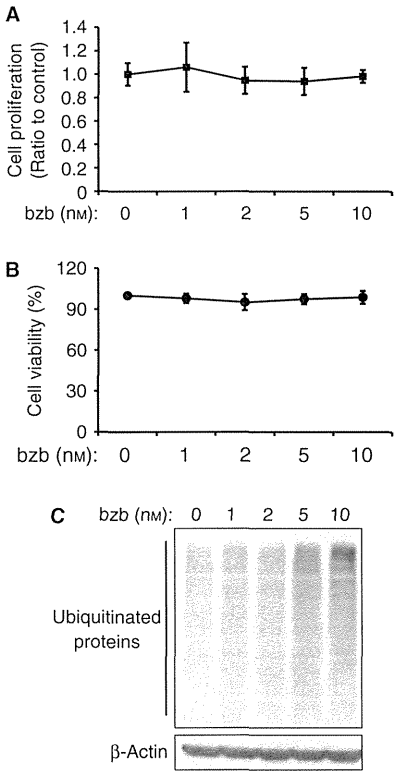

Fig. 1. Effects of bortezomib on the proliferation, viability and proteasome activity of MPLD22 cells. (A, B) Bortezomib did not affect the proliferation and viability of MPDL22 cells. MPDL22 cells were exposed to vehicle control [dimethylsulfoxide (DMSO)] or 1–10 nM bortezomib for 24 h, and cell proliferation and viability were examined using the WST-1 assay (A) and Trypan Blue exclusion (B), respectively. Data represent the mean and SD of three independent experiments. (C) Bortezomib increases the accumulation of ubiquitinated target proteins in MPDL22 cells. MPDL22 cells were incubated with bortezomib at the indicated doses for 5 d, and ubiquitination of target proteins and β-actin in cells were assessed by immunoblotting using anti-ubiquitin and anti-β-actin IgGs. bzb, bortezomib.

We next analyzed the effects of bortezomib on the ubiquitination of target proteins in MPDL22 cells. MPDL22 cells were treated with bortezomib and ubiquitination of target proteins was assessed by immunoblotting. As shown in Fig. 1C, bortezomib increased the mass of protein present in the high-molecular-weight region of the ubiquitin smear, which represents poly-ubiquitination of target proteins. This suggests that bortezomib suppresses the proteasome activity of MPDL22 cells.

Bortezomib stimulates cytodifferentiation of PDL cells

To evaluate the effects of bortezomib on the cytodifferentiation of MPDL22 cells, MPDL22 cells were cultured in mineralization medium with 10 nM bortezomib for 6 or 11 d. Gene expression of the extracellular matrix components and osteoblastic transcriptional factors was then assessed by real-time PCR. Bortezomib significantly enhanced expression of *ALPase* and osteopontin mRNAs during the 6-d incubation period (Fig. 2A). Following a longer period of incubation with bortezomib (11 d), a significant increase was observed in the expression of *ALPase*, *Bsp*, osteopontin and *Runx2* mRNAs (Fig. 2A). To evaluate, in more detail, the effects of bortezomib on the cytodifferentiation of PDL cells, we cultured HPDL cells with 10 nM bortezomib for 25 d. Bortezomib significantly enhanced the expression of osteopontin and *BSP* mRNAs (Fig. 2B). These data suggest that bortezomib stimulates cytodifferentiation in PDL cells.

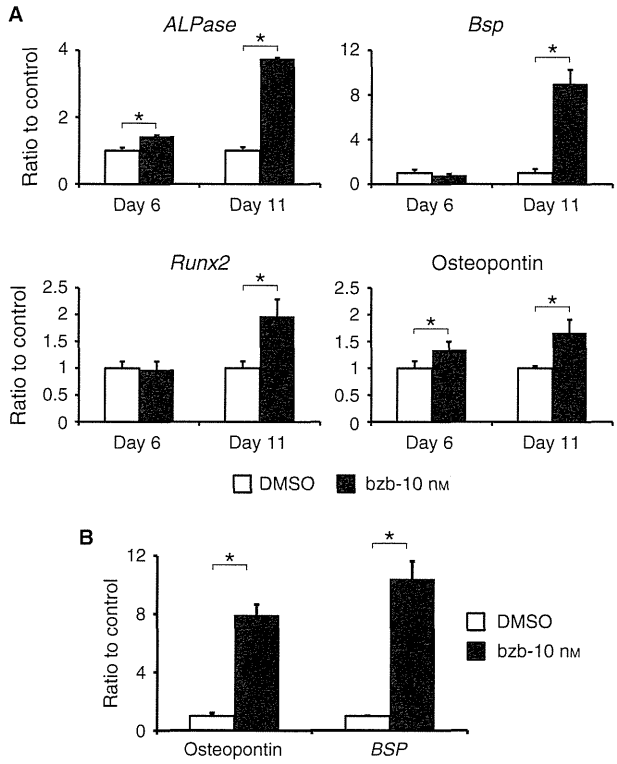

Fig. 2. Bortezomib increased calcification-related expression of tissue nonspecific alkaline phosphatase isoenzyme (*ALPase*), bone sialoprotein (*Bsp*), osteopontin and *Runx2* mRNAs in MPDL22 cells. (A) MPDL22 cells were incubated with 10 nM bortezomib for 6 or 11 d. The expression of *ALPase*, *Bsp*, osteopontin and *Runx2* mRNAs was investigated by real-time PCR. The relative expression of each gene was normalized to the expression levels of glyceraldehyde-3-phosphate dehydrogenase (*Gapdh*). Data represent the mean and SD of three independent experiments. $*p < 0.05$. (B) Human periodontal ligament (HPDL) cells were cultured with 10 nM bortezomib for 25 d. The expression of osteopontin and *BSP* mRNAs was assessed by real-time PCR. The relative expression of each gene was normalized to the expression levels of hypoxanthine-guanine phosphoribosyltransferase (*HPRT*). Data represent the mean and SD of three independent experiments. $*p < 0.05$ bzb, bortezomib.

Bortezomib enhances mineralization of MPDL22 cells

We cultured MPDL22 cells with bortezomib for 7, 11 and 17 d and then assessed the formation of calcified nodules by Alizarin Red staining. No calcified nodules were formed during the 7-d period of incubation (Fig. 3A, top row and 3B, closed bar). When the cells were incubated with bortezomib for 11 or 17 d, bortezomib increased calcified-nodule formation, compared with controls, in a dose-dependent manner (Fig. 3A, middle and bottom rows and 3B, open and hatched bars). These data suggest that bortezomib enhances mineralization of MPDL22 cells.

Bortezomib accumulates cytosolic and nuclear β-catenin

Use of the proteasome inhibitor, bortezomib, results in the intracellular accumulation of a number of target proteins and the activation of several signaling pathways. Wnt signaling is known to play an important role in controlling the osteoblastic differentiation of mesenchymal stem cells (15). Beta-catenin is a pivotal signaling molecule of the Wnt signaling pathway and is degraded by the ubiquitin proteasome system. Following the inhibition of ubiquitin-mediated degradation of β-catenin by bortezomib, β-catenin was stabilized and accumulated in the cytosol and then translocated to the nucleus (16). To evaluate the effects of bortezomib on the cytosolic accumulation and nuclear translocation of β-catenin in MPDL22 cells, MPDL22 cells were incubated with bortezomib for 5 d. The cytosolic accumulation and nuclear translocation of β-catenin were then assessed by immunoblotting. As shown in Fig. 4A, bortezomib increased the cytosolic accumulation of β-catenin in MPDL22 cells. Similarly, bortezomib enhanced nuclear translocation of β-catenin in MPDL22 cells (Fig. 4B),

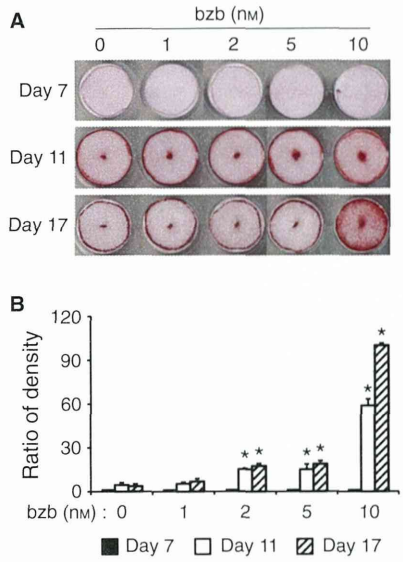

Fig. 3. Bortezomib increased calcified-nodule formation of MPDL22 cells. (A) Effect of bortezomib on calcified-nodule formation in MPDL22 cells was examined by Alizarin Red staining following 7, 11 and 17 d of cell culture. (B) The relative intensity of Alizarin Red staining was examined by image analysis. These data were quantified and normalized to the Alizarin Red staining of the vehicle control. Data represent the mean and SD of three different areas of the image. $*p < 0.05$ compared with vehicle control at the same time point of incubation. bzb, bortezomib.

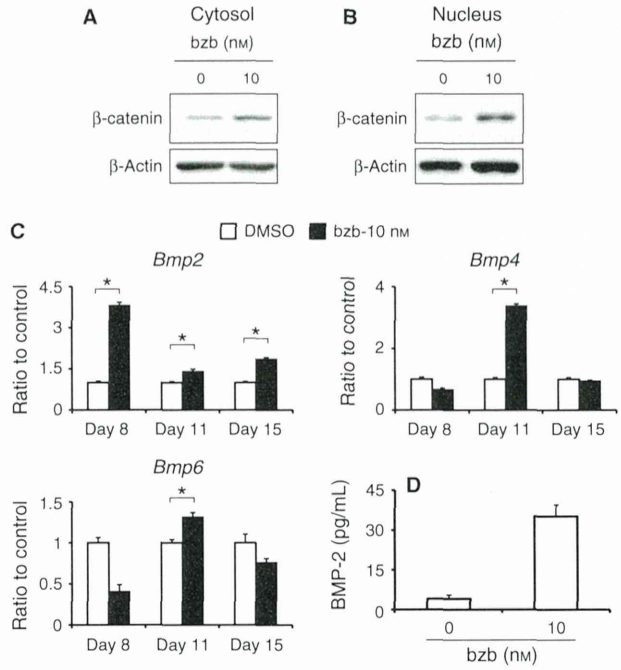

Fig. 4. Bortezomib induced the accumulation of cytosolic and nuclear β-catenin and increased the expression of bone morphogenetic protein (*Bmp*)-*2*, *-4* and *-6* mRNAs in MPDL22 cells. (A, B) MPDL22 cells were incubated for 5 d in mineralization medium with bortezomib, and cytosolic accumulation (A) and nuclear translocation (B) of β-catenin were analyzed by immunoblotting with anti-β-catenin or anti- β-actin IgGs. (C) MPDL22 cells were exposed to bortezomib for 8, 11 and 15 d and the expression of *Bmp-2*, *-4* and *-6* mRNAs were assessed by real-time PCR. The relative expression of each gene was normalized to the expression levels of glyceraldehyde-3-phosphate dehydrogenase (*Gapdh*). Data represent the mean and SD of three independent experiments. $*p < 0.05$. (D) MPDL22 cells were incubated with bortezomib for 24 d and the expression of BMP-2 protein was assessed by ELISA. Data represent the mean and SD of four independent experiments. $*p < 0.05$. bzb, bortezomib.

suggesting that bortezomib enhances cytosolic accumulation and nuclear translocation of β-catenin in MPDL22 cells.

Bortezomib increases expression of *Bmp-2,-4* and *-6* mRNAs and the levels of BMP-2 protein in MPDL22 cells

A number of studies have demonstrated that BMP-2, -4 and -6, which are among the most potent cytokines to stimulate osteoblastic differentiation and bone formation, induce cytodifferentiation and mineralization of PDL cells (17–20). The accumulation and subsequent nuclear translocation of β-catenin increases the expression of BMP-2, -4 and -6 in mesenchymal cells and osteoblastic precursor cells (21–23). To analyze the effects of bortezomib on the expression of BMP-2, -4 and -6, MPDL22 cells were treated with bortezomib for 8, 11 or 15 d. The expression of *Bmp-2*, *-4* and *-6* mRNAs were then assessed by real-time PCR. Bortezomib significantly increased the expression of *Bmp-2*, *-4* and *-6* mRNAs in MPDL22 cells during the 11-d incubation period and increased expression of *Bmp2* mRNA during the 8-, 11- and 15-d incubation periods (Fig. 4C). These data indicate that bortezomib-induced cytodifferentiation and mineralization of MPDL22 cells may depend on the increase of *BMP-2, -4 and -6* expression in MPDL22 cells. Furthermore, it was demonstrated that treatment of MPDL22 cells with bortezomib significantly increased the levels of BMP-2 protein (Fig. 4D).

Bortezomib enhances the BMP-2-induced cytodifferentiation and mineralization of MPDL22 cells

We next analyzed the effects of bortezomib on BMP-2-induced cytodifferentiation and mineralization in MPDL22 cells. MPDL22 cells were cultured with or without bortezomib in the presence or absence of BMP-2, and the expression of calcification-related genes was assessed by real-time PCR. We found that bortezomib enhanced the BMP-2-induced expression of *Bsp* and osteopontin mRNAs (Fig. 5). We then investigated the effect of bortezomib on calcified-nodule formation in BMP-2-stimulated MPDL22 cells. Alizarin Red staining revealed that bortezomib did not increase calcified-nodule formation

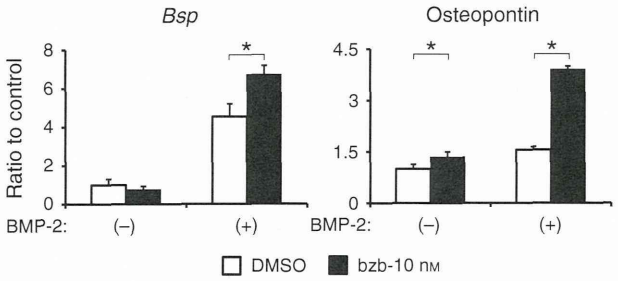

Fig. 5. Bortezomib enhanced bone morphogenetic protein (BMP-2)-induced expression of bone sialoprotein (*Bsp*) and osteopontin mRNAs in MPDL22 cells. MPDL22 cells were exposed to 10 nM bortezomib in the presence or absence of 50 ng/mL of BMP-2 for 6 d. The expression of *Bsp* and osteopontin mRNAs was assessed by real-time PCR. The relative expression of each gene was normalized to the expression levels of glyceraldehyde-3-phosphate dehydrogenase (*Gapdh*). Data represent the mean and SD of three independent experiments. $*p < 0.05$. bzb, bortezomib; DMSO, dimethylsulfoxide.

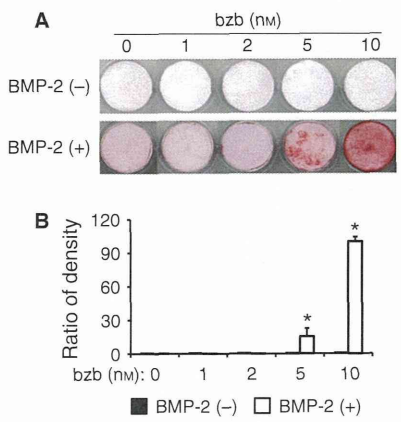

Fig. 6. Bortezomib increased bone morphogenetic protein (BMP-2)-induced calcified-nodule formation of MPDL22 cells. (A) MPDL22 cells were incubated with bortezomib in the presence or absence of 50 ng/mL of BMP-2 for 6 d. Calcified-nodule formation was assessed by Alizarin Red staining. (B) The relative intensity of Alizarin Red staining was examined by image analysis. These data were quantified and normalized to the level of Alizarin Red staining of the vehicle control. Data represent the mean and SD of three different areas of the image. $*p < 0.05$ compared with vehicle control. bzb, bortezomib.

during a 6-d incubation period in the absence of BMP-2 (Fig. 6A top row, 6B closed bar), whereas bortezomib increased calcified-nodule formation, in a dose-dependent manner, in the presence of BMP-2 (Fig. 6A bottom panel, 6B open bar). These data indicate that bortezomib enhances BMP-2-induced cytodifferentiation and mineralization of MPDL22 cells in a dose-dependent manner.

Discussion

In the present study, we demonstrated that bortezomib increased the accumulation of ubiquitin-targeted proteins in MPDL22 cells in a dose-dependent manner. Moreover, bortezomib enhanced expression of calcification-related genes and calcified-nodule formation in MPDL22 cells. Its mechanism of action was partially through an increase in the cytosolic accumulation and nuclear translocation of β-catenin, leading to the increase in expression of *Bmp-2*, *-4* and *-6* mRNAs. In addition, we showed that bortezomib acts through the enhancement of BMP-2-induced cytodifferentiation and mineralization of MPDL22 cells, suggesting that bortezomib may be efficacious in the regeneration of periodontal tissue.

Bortezomib is an effective compound in the treatment of multiple myeloma. For the treatment of multiple myeloma, 1.3 mg/m^2 of bortezomib is administered twice weekly to patients (4). The mean plasma concentration of bortezomib for this treatment, when administered either subcutaneously or intravenously, is approximately 1–3 ng/mL (3–8 nM) (24). In the present study, we concluded that 10 nM bortezomib, which is, in general, the most effective concentration when used clinically, enhanced the cytodifferentiation and mineralization of PDL cells, and concentrations of bortezomib of > 10 nM resulted in cytotoxic effects in PDL cells (data not shown). Interestingly, while 10 nM bortezomib enhances the expression of osterix and osteocalcin mRNAs and calcified-nodule formation, concentrations of bortezomib of > 20 nM were shown to suppress their expression and formation in the mouse osteoblastic precursor cell line MC3T3-E1 cells (25). Taken together, these data indicate that 10 nM bortezomib might be the optimal concentration for periodontal tissue regeneration. It is worth noting that while bortezomib is currently administered only subcutaneously or intravenously, a novel oral administration of the bioactive proteasome inhibitor, MLN9708, is under investigation and has the potential to alleviate osteolytic bone disease (26).

A number of studies have demonstrated that several chemical compounds prevent bone resorption caused by the progression of periodontitis. The compound kavain is known to prevent the degradation of IκB, leading to the inhibition of nuclear factor-κB and tumor necrosis factor-α activity (27). This compound inhibits bone loss in a *Porphyromonas gingivalis*-soaked ligature-induced periodontitis mouse model (28). Histone deacetylase inhibitors 1179.4b and MS-275 also reduce the bone loss in mice inoculated with *P. gingivalis* by repressing inflammatory cytokines, such as tumor necrosis factor-α (29). These compounds demonstrate anti-inflammatory effects, which lead to the inhibition of bone resorption in a periodontitis murine model. In a manner similar to these compounds, bortezomib inhibits the ubiquitin-mediated degradation of IκB, leading to the inhibition of tumor necrosis factor-α activity (30), and induces cytodifferentiation and mineralization in PDL cells. These results, including those presented within this study, suggest the possible use of such chemical compounds for periodontal therapy in the future.

Bortezomib directly enhances β-catenin cytosolic accumulation and nuclear translocation. In the absence